Lasers in Surgery and Medicine 26:292–301 (2000)

Comparison Between Isotropic and Nonisotropic Dosimetry Systems During Intraperitoneal Photodynamic Therapy

Teodor G. Vulcan, PhD,[1,2] Timothy C. Zhu, PhD,[2] Carmen E. Rodriguez,[2] Alex Hsi, MD,[2] Douglas L. Fraker, PhD,[3] Paul Baas, MD, PhD,[4] Lars H.P. Murrer, PhD,[5] Willem M. Star, PhD,[5] Eli Glatstein, MD,[2] Arjun G. Yodh, PhD,[1,2] and Stephen M. Hahn, MD[2]*

[1]Department of Physics and Astronomy University of Pennsylvania, Philadelphia, Pennsylvania 19104-4283
[2]Department of Radiation Oncology, University of Pennsylvania, Philadelphia, Pennsylvania 19104-4283
[3]Department of Surgery, University of Pennsylvania, Philadelphia, Pennsylvania 19104-4283
[4]Department of Medical Oncology, The Netherlands Cancer Institute, 1066 CX Amsterdam, the Netherlands
[5]Department of Clinical Physics, Dr. Daniel den Hoed Cancer Center, 3008 AE Rotterdam, the Netherlands

Background and Objective: **On-line monitoring of light fluence during intraperitoneal photodynamic therapy (IP PDT) is crucial for safe light delivery. A flat photodiode-based dosimetry system is compared with an isotropic detector-based system in patients undergoing IP PDT.**
Study Design/Materials and Methods: **Flat photodiodes and spherical detectors were placed side by side in the abdomen, for simultaneous light dosimetry in 19 patients. Tissue phantom experiments were performed to provide a preliminary estimate of the tissue optical properties of the peritoneum.**
Results: **The conversion factor between systems for 630-nm light was found to be 1.7 ± 0.12. The μ_{eff} of the tissues in the abdomen is estimated to vary between 0.5 cm^{-1} to 1.4 cm^{-1} assuming a $\mu_s' = 7$ cm^{-1}.**
Conclusions: **The measured conversion factor should allow for comparison of light fluences with future clinical protocols that use an isotropic-based detector system. Differences in the optical properties of the underlying tissues may contribute to the variability in light measurements. Lasers Surg. Med. 26:292–301, 2000.** **© 2000 Wiley-Liss, Inc.**

Key words: cancer; isotropic; photodynamic therapy; photodiode; light diffusion

INTRODUCTION

Intraperitoneal photodynamic therapy (IP PDT) is an investigational cancer treatment for patients with incurable disseminated intraperitoneal malignancies including gastrointestinal cancers, sarcomas, and recurrent ovarian cancer [1,2]. A Phase I trial of IP PDT was performed at the National Cancer Institute, and encouraging clinical results were obtained [1,2]. This trial defined the maximally tolerated dose of Photofrin® and light. The dose-limiting toxicities appeared to depend on light fluence (measured with the flat photodiode dosimetry system) and wavelength [1]. It is clear from the results of this trial that treatment of the peritoneal cavity with visible light is a complicated task and that on-line light dosimetry is required [1,2]. The importance of on-line light dosimetry is also supported by the results of preclinical studies of IP PDT [3,4].

PDT effectiveness depends on several factors [5–7]. One of these factors is a reliable measure-

*Correspondence to: Stephen M. Hahn, MD, Department of Radiation Oncology, Hospital of the University of Pennsylvania, 2 Donner, 3400 Spruce Street, Philadelphia, PA 19104-4283.

Accepted 12 October 1999

ment of the light fluence delivered to target tissues. Such measurements are essential for the assessment of PDT efficacy and toxicity. Because the variability in tissue optical properties is often large [8], there may be a large variability in light fluences delivered to the superficial tissues. Only with accurate measurements of light fluences will it be possible to deliver safe, standardized PDT treatments.

The technique of IP PDT was developed by Sindelar et al. [2]. It consists of intravenous administration of Photofrin® 48 hours before the debulking surgery, followed by the application of green light (532 nm) to the surface of the bowels and mesentery, and application of red light (630 nm) to the remainder of the peritoneal surfaces. In the Phase I trial [1], real time light dosimetry was accomplished with flat photodiodes placed at representative locations in the patient's abdomen. These photodiodes measured incident light irradiance but were much less sensitive to scattered light and, thus, probably underestimated the total fluence delivered to the tissues.

We have initiated a Phase II trial of IP PDT at the University of Pennsylvania by using the maximally tolerated dose of Photofrin® and light established in the Phase I trial. In this trial, the prescribed fluences of light are based upon the measurements from the flat photodiode dosimetry system. It is our hypothesis that a spherical detector-based dosimetry system would more accurately measure the total light fluence delivered to sites within the peritoneal cavity during IP PDT [9–12]. Therefore, a comparison of the flat photodiode system with a spherical detector-based dosimetry system was initiated in 19 patients treated on a prospective Phase II study of IP PDT. In this study, we report the results of this comparison and determine a factor that will allow conversion of prescribed light fluences between the two systems. A preliminary estimate of the heterogeneity of tissue optical properties within the abdomen has also been made based on the dosimetry measurements.

MATERIALS AND METHODS

Intraperitoneal PDT

Nineteen patients with disseminated intraperitoneal malignancies were entered on a stratified Phase II trial of IP PDT. The clinical trial and the comparison of two different dosimetry systems were approved by the Institutional Review Board at the University of Pennsylvania. Patients were entered into one of three strata based on their diagnosis: ovarian cancer, sarcoma, or gastrointestinal malignancies. Nine patients with sarcomas, four patients with ovarian cancer, and six patients with gastrointestinal cancers form the basis of this evaluation. Photofrin® 2.5 mg/kg (purchased from QLT, Ltd., Vancouver, Canada) was administered intravenously to each patient. Forty-eight hours later, the patient was taken to the operating room for debulking surgery. All gross disease was resected to a thickness of 5 mm or less. The prescribed light fluence and light delivery technique (including the use of Intralipid) are the same as that used in the Phase I clinical trial performed at the National Cancer Institute [1,2], in which the flat photodiodes were exclusively used for light dosimetry. Because the main objective of the ongoing Phase II clinical trial is to determine the efficacy of IP PDT as delivered in the Phase I trial (by using the same light delivery technique), light fluence is prescribed based on measurements made with the flat photodiode system.

The laparotomy was performed in a surgical suite at the Hospital of the University of Pennsylvania in which the room lights were covered with filters to minimize unwanted activation of the photosensitizing drug at wavelengths below 550 nm, thereby reducing light absorption in the blue-green range.

After successful debulking of the disease sites, light was administered as follows: 532 nm green light, 2.5 J/cm^2 applied to surface of the mesentery, small and large bowel; and 630 nm red light, 5 J/cm^2 applied to the stomach and omental bursa; 7.5 J/cm^2 to the surface of the liver, spleen, and diaphragm; and 10 J/cm^2 to the peritoneal (paracolic) gutters and pelvis. Boosts to areas of gross disease were given with either 532-nm green light with a fluence of 1.0 to 3.0 J/cm^2, or 630-nm red light with a fluence of 3.0–10.0 J/cm^2. The average fluence rate for all treatments at the tissue surface was less than 150 mW/cm^2.

The mesentery, large bowel, and small bowel were treated with a flat cut optical fiber perpendicular to the tissue, held by a clamp at a distance of 50–75 cm from the patient. The light fluence was monitored by means of a sterile mobile flat photodiode that was placed in the light field to provide real time readings of the incident light delivered.

After the delivery of 532-nm light to the bowel surfaces and mesentery, 630-nm light was

applied to the remainder of the peritoneal cavity. Five sterile, flat photodiodes were sewn to the wall of the peritoneal cavity in the following sites: right upper quadrant, superior to the liver on the peritoneal surface of the diaphragm (RUQ); left upper quadrant, superior to the spleen on the peritoneal surface of the diaphragm (LUQ); right peritoneal gutter, on the peritoneal surface of the abdominal wall (RG); left peritoneal gutter, on the peritoneal surface of the abdominal wall (LG); and pelvis, on the peritoneal surface of the abdominal wall anterior to the bladder (PEL). For the purposes of comparing the light fluences measured with the two dosimetry systems, spherical (isotropic) detectors were sewn next to the flat photodiodes in four sites. The distance between each flat detector and its corresponding spherical detector was no more than 1 cm along the tissue surface. The spherical detectors were placed in sterile polyethylene intravenous tubing filled with saline to match the refractive index of the surrounding medium as previously described [11].

Before 630-nm light delivery, the abdomen was filled with a dilute solution of Intralipid (0.01%), in sterile lactated Ringer's solution. The light was delivered to the diaphragmatic surfaces, the liver, the splenic bed, the abdominal wall, the stomach, and the pelvis by using an optical fiber sheathed within a modified endotracheal tube. The balloon cuff was inflated and filled with 0.1% Intralipid. This device provided a more uniform light field compared with a bare fiber and protected tissues from light-induced thermal effects. During the illumination, light fluences were monitored simultaneously with both the flat photodiodes and the spherical detectors. The light fluence measured by the flat photodiodes was used to deliver the prescribed fluence as required by the clinical protocol. Measurements from the spherical detectors were recorded for the purposes of comparing the dosimetry systems.

The patients received one course of light therapy at the time of surgery. After administration of the light and its completion, and before abdominal closure, the sterile flat photodiodes and the isotropic detectors were removed from the abdomen and were passed from the table.

Laser System

The laser system used for IP PDT was an 81XP Model 820 NdYAG KTP laser with 40 W maximal power at 532 nm, and a 600 Series DYE Module with 7 W maximal power at 630 nm (purchased from Laserscope Surgical Systems, Inc., San Jose, CA). The output of the laser was verified by using a Coherent LabMaster Ultima digital power with calibration traceable to the National Institute of Standards.

Flat Photodiode-Based Dosimetry System

The flat photodiode dosimetry system used in the Phase I clinical trial of IP PDT was borrowed from the Radiation Oncology Branch at the National Cancer Institute (NCI), Bethesda, MD, and has been previously described [13]. It consists of a set of eight photodiodes connected to an analog-to-digital converter, which is interfaced to a personal computer (PC). The newest version of the software was also supplied by NCI. The system measures incident light irradiance (mW/cm^2) and total incident light fluence (time integrated irradiance, also called radiant exposure [12], in J/cm^2) accumulated at the site where the diode is placed. The calibration procedure is similar to the method described in Phase I trial [2]. The original determination of the maximally tolerated light fluence for the earlier clinical trials was based on the use of the flat photodiode-based dosimetry system, which was calibrated with green light at 515 nm. To maintain the continuity of the treatment protocols, the photodiodes in the present clinical trial were also calibrated with green light with a wavelength of 532 nm. The difference in calibration due to the smaller sensitivity of the silicon photodiode at 515 nm versus 532 nm is less than 5%. Collimated 532-nm green light was used in the calibration by recording two known values of the irradiance in air and the corresponding voltages for each of the eight photodiodes. The sensitivity of the flat photodiodes was larger at 630 nm than at 532 nm. Therefore, the voltage measurements from the flat photodiodes are 35% to 45% larger for the 630-nm light compared with 532 nm light for the same fluence rate.

Spherical (Isotropic) Detector-Based Dosimetry System

The spherical (isotropic) detector-based dosimetry system (built in the laboratory of Dr. Willem Star by Dr. Lars Murrer, and provided by Dr. Star and Scotia Pharmaceuticals, Ltd., Guildford, United Kingdom) is similar to the apparatus described by Baas et al. [11]. The system consists of four photodiodes/operational amplifiers (Photop UDT-455, Graseby Electronics, Orlando, FL), four SMA connectors for the spherical optical fiber detectors, an analog-to-digital converter module and an integrating sphere calibration module. The

spherical detectors, manufactured by CardioFocus, Inc. (West Yarmouth, MA) consist of optical fibers with a spherical bulb at the tip [10]. The bulb is made of a highly diffusing material, and the radius of the bulb (about 0.5 mm) is more than 10 times larger than the photon transport mean free path length in the material. The other end of the fiber is connected to its corresponding photodiode-operational amplifier in the AD converter module. The system is connected to a Toshiba notebook computer by means of a parallel port connection. The software (TiePie Engineering, Sneek, The Netherlands) enables real-time monitoring of light fluence rate and cumulated fluence, as well as relative calibration verification by using the integrating sphere calibration module. The absolute calibration of the system was verified by independently measuring collimated 630-nm light in air and water and was found to be within 5%.

Considerations on the Calibration and Response of the Detectors

The principle of the isotropic (spherical) detector is described in detail by Marijnissen and Star [10]. Light impinging on the bulb from any direction is multiply scattered before it contributes to the light that enters the optical fiber. Thus, the scattering bulb acts as a near isotropic light integrator. The spherical detector measures the radiant energy fluence rate ϕ, whereas the flat detector measures the irradiance E [10]. The irradiance, E (W/m^2), at any given point on a surface is the radiant power (or energy flux) incident on an infinitesimal element of the surface centered on that point, divided by the area of the surface element. The fluence rate, ϕ (W/m^2), at any given point in space is the radiant power incident on an infinitesimal sphere centered on that point, divided by the cross-sectional area of the sphere.

The detector output voltage V is proportional to the fluence rate ϕ (for the spherical detector), or irradiance E (for the flat detector), at the detector location, i.e., $(V - V_{dark}) = K \bullet (\phi \text{ or } E)$. Here, V_{dark} is the "dark" voltage (corresponding to no incident light), and K is a proportionality constant. A similar relation exists between $V_{cal}$and the calibrated reference light fluence rate or irradiance $(\phi_{cal} \text{ or } E_{cal})$. Thus, the measured fluence rate or irradiance is:

$$(\phi \text{ or } E)_{meas} = (\phi \text{ or } E)_{cal} \cdot (V - V_{dark})/(V_{cal} - V_{dark}). \quad (1)$$

The isotropic detector system has a built-in integrating sphere with light sources that provide ϕ_{cal}. Before each clinical use of the system, an absolute in-air calibration is performed by measuring and recording V_{cal} and V_{dark} for each fiber optic detector. The constant ϕ_{cal} was determined as part of the original calibration of the system by measuring the response of the system in air by using a collimated light beam (at the operating wavelength of 630 nm for the IP cases). A correction factor for spherical detector measurements in water was determined afterward; it accounts for the mismatch of the material refractive indices and was verified by direct measurements of known fluence rates (or irradiances) of collimated beams in water.

For a collimated light source the fluence rate at the tip of the optical fiber is equal to the irradiance of the collimated beam at the same location [10], i.e., $\phi_{spherical} = E_0$. Here E_0 is the irradiance that would be measured with a calibrated flat detector placed with its surface perpendicular to the incident wave. The fluence rate for a spherical detector placed near the surface of an infinite perfectly diffuse reflecting surface illuminated by a collimated beam with propagation vector perpendicular to the surface is $\phi_{spherical} = 3\ E_0$. In this relation, one E_0 comes from the direct beam, and $2E_0$ represents the contribution of the diffuse reflecting surface [10]. Similarly, it can be proven that the contribution of the same diffuse reflecting surface to the irradiance measured with a flat detector facing this diffuse reflecting surface is $E_{flat} = E_0$. If the definition for fluence rate is applied to a completely isotropic diffuse light field (as it is in an ideal integrating sphere), then the result gives four times the irradiance measured with the flat detector with surface normal fixed along any direction [10], i.e., $\phi_{spherical} = 4\ E_0$.

Hence, for two ideal flat and spherical detectors placed in the same location in an arbitrary light field, the spherical detector will read a factor of 1 to 4 times larger than the flat detector. The actual factor depends on the optical properties and geometry.

The ratio of the spherical and flat detector readings, i.e., (Spherical)/(Flat), located on the surface of a semi-infinite tissue medium and illuminated from above with a homogeneous parallel light beam depends on the diffuse reflectance R_d, i.e.,

$$\text{(Spherical)/(Flat)} = 1 + 2\ R_d. \quad (2)$$

If we assume that the tissue surface is a Lamber-

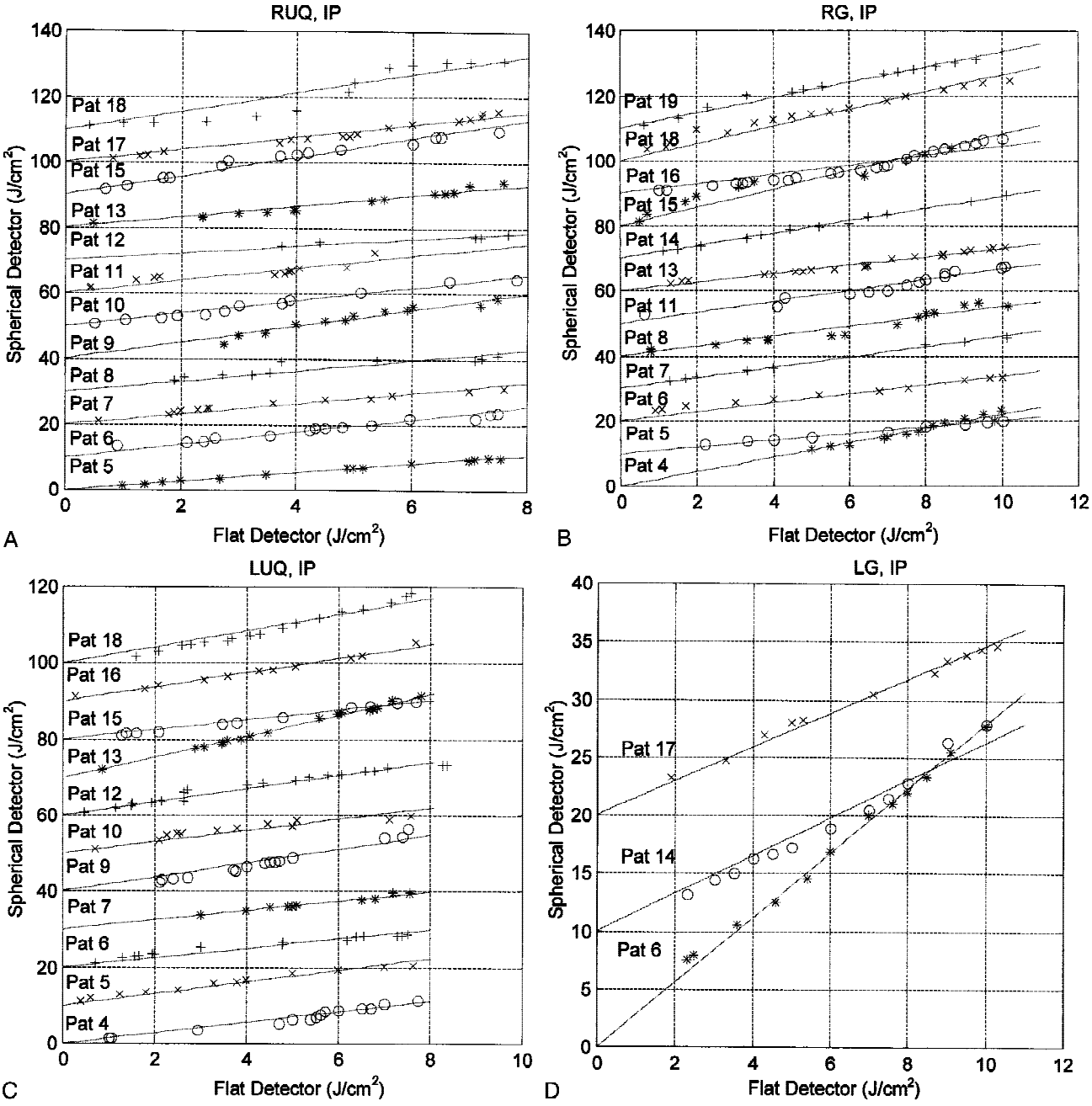

Fig. 1. A comparison between spherical and flat detector reading for patients undergoing intraperitoneal photodynamic therapy, demonstrating both the final and intermediate data points during treatment. The lines are a fit to $y = a \times x$. The symbols represent measured values for individual patients and are shifted 10 J/cm² to show the intermediate values for each individual patient. **A:** Values for detectors placed in the right upper quadrant (RUQ); the weighted average of a is 1.64 ± 0.17. **B:** Values for detectors placed in the right gutter (RG); the weighted average of a is 1.68 ± 0.17. **C:** Values for detectors placed in the left upper quadrant (LUQ); the weighted average of a is 1.64 ± 0.14. **D:** Values for detectors placed in the left gutter (LG); the weighted average of a is 1.93 ± 0.42. **E:** Values for detectors placed in the pelvis; the weighted average of a is 1.83 ± 0.21.

tian surface for angles less than 30° (14). The expression for R_d is obtained using the diffusion theory (15):

$$R_d = \frac{a'}{2}\left(1 + e^{-(4/3)A\sqrt{3(1-a')}}\right)e^{-\sqrt{3(1-a')}}. \qquad (3)$$

Here a' is the transport albedo: $a' = \mu_s'/(\mu_a + \mu_s')$, and A is an internal reflection parameter which is a function of the ratio of the refraction indices of the two media (15). We will compare theory to phantom experiments later in the study.

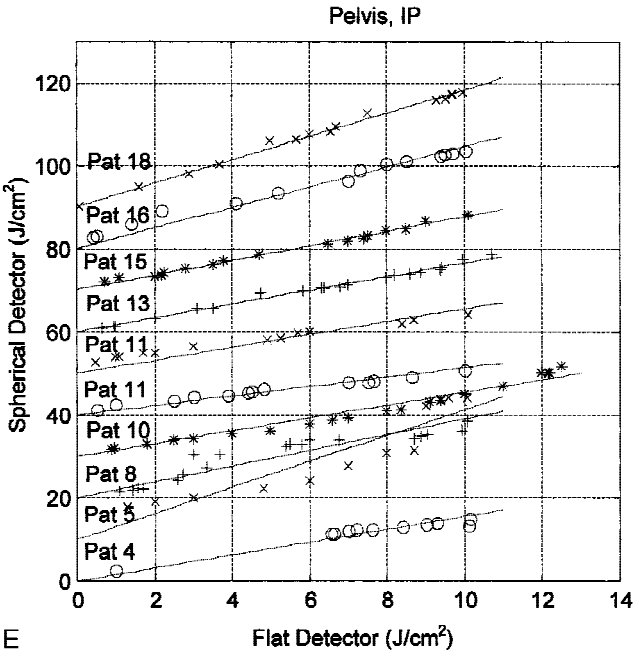

Fig. 1. (Continued)

In Vivo Comparison of the Two Dosimetry Systems

Light measurements for 630-nm treatments were made for all 19 patients reported. For patients 1–3, only the final (cumulative) fluences were recorded without intermediate values. The data from these three patients were not used for the calculation of the tissue heterogeneity but were included for determination of the conversion factor. Data from the intermediate and cumulative light fluence measurements made with the isotropic detector-based system were plotted against the fluences measured with the flat photodiode-based system (Fig. 1). A straight line through the data points corresponds to the least square fit of the data. The slope of this line represents the conversion factor for the two dosimetry systems for each individual patient. The standard error for the slope was determined by calculating the mean square difference between measured and predicted data [16]. The coefficient of correlation R^2 varies between 0 and 1 and provides an assessment of how well the data fits a linear model [16]. For each site, the error weighted mean and standard deviation of the mean is calculated.

Phantom Experiments

The phantom experiments attempted to reproduce the conditions encountered in vivo. The primary goal of these measurements was to provide an estimate of the optical property variations required to explain observed in vivo variations between the spherical and flat detector measurements. The systematic errors (probably due to the cumulated effects of the detector's shadow on the finite diffusive reflective surface, the fluctuations of the power source, the calibration errors, etc.) were estimated to be within 15%.

For these experiments, flat and spherical detectors were placed side by side in a water tank above a sealed plastic bag containing solutions of Intralipid and ink of known concentration (optical parameters μ_a and μ_s'). Additional Intralipid solution (diluted to 0.01%) was poured into the tank, such that the surface of the liquid was about 10–15 cm above the detectors. Both dosimetry systems were recording, while a light source consisting of an optical fiber with a spherical diffuser was moved back and forth in the liquid above the detectors. Several plastic bags with different phantom solutions corresponding to different optical properties were placed under the detectors. The absorption and scattering coefficients of the phantom samples were measured independently by diffuse wave propagation techniques (e.g., [17]). To maintain the same conditions as those existing during in vivo measurements, the flat detector system was calibrated at 532 nm, and the spherical detector system at 630 nm.

RESULTS

In Vivo Comparison of the Two Dosimetry Systems

The comparison of data taken with both light dosimetry systems in IP PDT patients with intermediate data points is displayed in Figure 1. The fluences measured with the spherical detector-based system are plotted against the fluences measured with the flat detector-based system for each patient at various treatment sites, including the RUQ (right upper quadrant), LUQ (left upper quadrant), RG (right gutter), LG (left gutter), and PEL (pelvis). Tables 1 and 2 summarize the data from all patients. In addition to calculating conversion factors for each patient, the data are analyzed according to treatment site. In some cases, a lower correlation between intermediary and the final data points was detected ($R^2 < 0.95$). These data are indicated by an asterisk after the patient number.

The conversion factor for the 630-nm red light treatment was found to be 1.7 ± 0.12. This number was obtained by using the error weighted average of the conversion factors for the five treatment sites (e.g., from Table 1, 1.64 ± 0.17, 1.64 ± 0.14, 1.68 ± 0.17, 1.93 ± 0.42, and 1.83 ± 0.21, at RUQ, LUQ, RG, LG, and PEL, respectively). If the error weighted average value of the final data points is calculated after eliminating the data from patients with a lower correlation between intermediary and final data points (from Table 1: 1.60 ± 0.18, 1.67 ± 0.11, 1.62 ± 0.13, 1.93 ± 0.42, and 1.97 ± 0.14), the average is the same, 1.73 ± 0.11.

Phantom Measurements and Estimate of Tissue Optical Properties

To maintain the same conditions as the in vivo measurements, the flat detector system was calibrated at 532 nm, and the spherical detector system at 630 nm. The results of the comparison of the two dosimetry systems in phantoms are shown in Figure 2 as a plot of the ratio (Spherical)/(Flat) versus μ_{eff} of the phantom (two values of μ_s': 7 cm^{-1} and 15 cm^{-1}, and several values for μ_a). The same figure shows theoretical curves derived by using equations 1 and 2 [14,15] for μ_s' of 7 cm^{-1} and 15 cm^{-1} and continuously varying μ_a. The phantom measurements allowed an estimate of the μ_{eff} in biological tissues that could explain the observed variations in the in vivo spherical detector measurements.

The first observation from the phantom measurements is that the fluence rate variability measured at the surface of phantoms with relatively large values of the scattering coefficients (e.g., in the published ranges for biological tissues, [7,8] is due mainly to variations of absorption, rather than scattering. In particular, pure Intralipid phantoms with μ_s' of 7 cm^{-1} and 15 cm^{-1} and the same absorption coefficient of μ_a = 0.023 cm^{-1}, exhibit relatively small differences in the fluence rate measured above their surface. But when μ_a is increased to 0.05 cm^{-1}, the change in fluence rate is relatively larger (e.g., the first three data points in the left upper corner of Fig. 2).

The ratio between the spherical and flat detector is a function of transport albedo [15]; it depends on both μ_s' and μ_a, rather than μ_{eff}, with the theoretical maximum of approximately 1.92 (0.64 multiplied by 3, where 0.64 is the wavelength correction factor for the flat detector) as demonstrated by the point in Figure 2 where the curves are converging. From the same curves in Figure 2, an estimate of μ_{eff} can be made, assuming μ_s' is approximately the same in different tissues. After all data points with a correlation coefficient of less than 0.95 are eliminated, the conversion ratio averaged over all sites is 1.7 ± 0.11. Assuming an μ_s' = 7 cm^{-1}, from the experimental data the range of μ_{eff} is predicted to vary between 0.5 to 1.4 cm^{-1}. A simple calculation based on these data suggests that the actual fluence rate 5 mm below the tissue surface may be varying by factors of 1.6 to 2.6 when μ_s' are 7 cm^{-1} and 15 cm^{-1}, respectively. If all of the data from Table 1 are included, these fluence rate variations would have been predicted to be even larger.

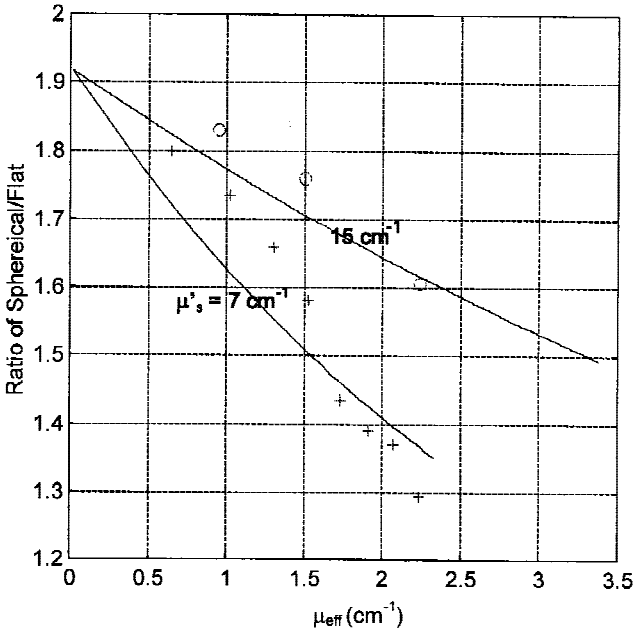

Fig. 2. Ratio of the spherical and flat detector measurements in phantoms of known absorption (μ_a) and scattering (μ_s) coefficients as function of effective attenuation coefficient μ_{eff}. Symbols are measured data: circles, μ_s = 15 cm^{-1}; plus signs, μ_s = 7 cm^{-1}. Solid lines are fit to equation (1). The fit corrects for the known calibration wavelength dependence of the flat detector.

DISCUSSION

IP PDT is an experimental treatment approach being evaluated for the treatment of patients with intraperitoneal malignancies that are incurable with present treatment techniques. The tissue geometry in the peritoneal cavity is extremely complex, which makes custom light delivery difficult. Furthermore, the doses for Photofrin® and light used in this trial represent the

TABLE 1. Summary of the Data Sets for the In Vivo Comparison of the Spherical Detector-Based Dosimetry System and Flat Photodiode-Based Dosimetry System in Patients 4 Through 19*

Patient number	Conversion factor	Standard deviation	Correl. coeff. (R^2)
RUQ			
5	1.34	0.06	1.00
6*	1.94	0.43	0.93
7*	1.60	0.39	0.92
8*	1.58	0.64	0.75
9*	2.48	0.68	0.94
10	1.94	0.28	0.98
11*	1.89	0.81	0.78
12*	1.07	0.32	0.85
13	1.62	0.40	0.95
15	2.86	0.54	0.96
17	1.88	0.35	0.97
18*	2.77	1.30	0.87
All data for RUQ	1.64	0.17	—
Data ($R^2 > 0.95$)	1.60	0.18	—
LUQ			
4	1.39	0.32	0.95
5*	1.54	0.31	0.94
6*	1.24	0.31	0.90
7	1.24	0.16	0.98
9*	1.83	0.70	0.92
10*	1.50	0.59	0.77
12	1.77	0.35	0.96
13	2.73	0.22	0.99
15	1.28	0.16	0.99
16	1.87	0.23	0.99
18*	2.14	0.69	0.94
All data for LUQ	1.64	0.14	—
Data ($R^2 > 0.95$)	1.67	0.11	—
RG			
4	2.22	0.51	0.95
5	1.03	0.15	0.97
6*	1.40	0.40	0.86
7	1.61	0.10	1.00
8*	1.53	0.43	0.93
11*	1.68	0.45	0.93
13	1.31	0.19	0.98
14	1.91	0.11	1.00
15*	2.83	0.81	0.89
16*	1.46	0.61	0.90
18*	2.65	0.56	0.94
19	2.36	0.39	0.98
All data for RG	1.68	0.17	—
Data ($R^2 > 0.95$)	1.62	0.13	—
LG			
6	2.79	0.21	0.99
14	1.63	0.38	0.96
17	1.46	0.14	0.99
All data for LG	1.93	0.42	—
Data ($R^2 > 0.95$)	1.93	0.42	—
PELVIS			
4*	1.55	0.46	0.88
5*	3.13	1.30	0.85
8*	1.89	0.69	0.86
10	1.54	0.31	0.97
11L*	1.55	0.49	0.82
11R*	1.13	0.24	0.93
13	1.65	0.16	0.99
15	1.76	0.15	0.99
16	2.45	0.44	0.96
18	2.83	0.24	0.99
All data for PELVIS	1.83	0.21	—
Data ($R^2 > 0.95$)	1.97	0.14	—
All sites	1.72	0.12	—
All sites ($R^2 > 0.95$)	1.73	0.11	—

*Data from patient numbers that are marked by an asterisk had a correlation coefficient (R^2, of <0.95).

maximally tolerated dose, which means they are close to doses that could lead to substantial toxicity. Based upon the theoretical considerations presented earlier in this manuscript, and the observed heterogeneity of tissue optical properties in the peritoneal cavity, we postulate that the isotropic detector-based dosimetry system would permit a more accurate assessment of the light fluence delivered to the superficial tissues.

The first objective of this work was to determine the conversion factor between the flat detector-based dosimetry system and the spherical detector-based dosimetry system. The conversion factor is 1.7 ± 0.12. It is our contention, therefore, that the spherical detector-based system represents a more accurate measure of the superficial 630-nm light fluence, and that the flat photodiode-based system underestimates the actual fluence delivered. A comparison of the conversion factors at different locations within the abdomen for the same patient and for different patients (Table 1) indicates a relatively large variability in the ratio of spherical detector measurements to flat photodiode measurements. This variability may be due to the heterogeneity of the optical properties of the tissues. The variability observed was not systematic with respect to individual patients, nor with respect to the location within the intraperitoneal cavity.

The differences in calibration between the systems cannot be used to explain the experimental findings. The flat photodiode-based dosimetry system is calibrated at 532 nm, whereas the spherical detector-based system is calibrated at 630 nm. The silicon photodiodes used in both dosimetry systems are 35% to 45% less sensitive at 532 nm than at 630 nm, depending on the individual photodiode used. The flat photodiode-based system overestimates the irradiance at 630 nm by about 35% to 45%, whereas the spherical detector-based system measures the actual fluence rate.

TABLE 2. Summary of the Data Sets for the *In Vivo* Comparison of the Spherical Detector-Based Dosimetry System and Flat Photodiode-Based Dosimetry System in Patients 1 Through 3

Patient number	RUQ	LG	RG	
1	8.6	10	10	Flat system (J/cm^2)
	30	20	20.74	Spherical system (J/cm^2)
2	7.637	10.309	10.238	Flat system (J/cm^2)
	11.08	11.43	22.78	Spherical system (J/cm^2)
3	7.5	10.02	10.32	Flat system (J/cm^2)
	9.75	11.63	22.43	Spherical/system (J/cm^2)

Several other factors may also account for the difference between the spherical and flat detector readings: (1) angular dependence of flat and isotropic detectors and the pattern of light source movement; (2) nonlinearity of the photodiodes (the flat detectors begin to saturate at high irradiance (~130 – 200 mW/cm^2); (3) placement error of the two detectors in the abdomen; (4) errors in the isotropic detector reading due to accidental air bubbles in the intravenous tubing.

Careful set-up and placement of the detectors was used to decrease any errors that might have resulted from factors 3 and 4 during treatment. Nonetheless, it is difficult to completely eliminate these factors as a possible source of error. Factors 1 and 2 likely account for some of the differences between the spherical and flat detector readings.

Variability in tissue optical properties is likely the major reason for the differences observed between the two dosimetry systems. The other objective of this study was to estimate the optical property heterogeneity of the tissues exposed to light in vivo during the IP PDT treatment, and from this to evaluate the validity of the assumptions regarding light penetration depth, an important component of the treatment efficacy. A comparison of the in vivo data with phantom measurements was made to evaluate for this possibility and to make an estimate of these properties. To make a comparison between the in vivo data and the phantom measurements, it was important to eliminate variations due to nonuniform light source movement and detector nonlinearity. A good correlation between the data points in a series is an indication that the flat and the spherical detector were under uniform light irradiation. Saturation of the flat detector during light delivery and nonuniformity of light source movement could introduce nonlinearities and, thus, a smaller correlation coefficient for intermediary data points with the cumulative data point. Therefore, the individual patient data sets with R^2 less than 0.95 were eliminated from the analysis of tissue optical properties. Approximately 40% of the data sets from Table 1 had a correlation coefficient less than 0.95 and were eliminated for the purpose of determining tissue heterogeneity.

For this assessment, we compared the light measurements of the flat and spherical detector dosimetry systems in vivo with similar measurements taken in phantoms of known optical properties. Our data show that, assuming an $\mu_s' = 7$ cm^{-1}, the range of μ_{eff} varies between 0.5 and 1.4 cm^{-1}. A calculation based on these data shows that the fluence rate 5 mm below the tissue surface may be varying by a factor of 1.6 simply as a result of the tissue optical property heterogeneity. If all of the data from Table 1 are analyzed (including patient data with an R^2 less than 0.95), an even greater degree of variability of light fluence is observed.

A conversion factor from the flat photodiode-based system to a spherical detector-based system has been determined from in vivo light measurements in patients with intraperitoneal malignancies. The conversion factor will be useful for "translating" light fluences prescribed in the present protocol with light fluences used in future protocols that use the spherical detector-based dosimetry system. It cannot be assumed, however, that application of the conversion factor in the current clinical protocol would, in fact, produce equivalent clinical results. Additional clinical experience with the spherical detector-based dosimetry system will be required before it can be accepted as a method of safely monitoring light fluence during IP PDT. Nonetheless, the conversion factor is useful for comparing clinical data previously generated from the flat photodiode system with future protocols that use a spherical detector-based system.

The flat photodiode-based dosimetry system has been useful for maintaining the continuity of treatment protocols for IP PDT. However, our data suggest that the flat photodiodes underestimate the actual light fluence at the tissue surface. The spherical detector-based dosimetry system provides a more accurate representation of the photons available for treatment and therefore, should be used for future treatment protocols. The clinical data from spherical detector measurements demonstrate a substantial degree of heterogeneity. Phantom experiments support the concept that part of the heterogeneity is due to

differences in the optical properties of the underlying tissues within the abdomen. This estimate of the optical properties of the abdominal structures is a first step in our ongoing effort to define better the light fluence delivered to tissues during clinical PDT. Given the heterogeneity observed in our study, the continued use of on-line in vivo light dosimetry during IP PDT is warranted.

REFERENCES

1. DeLaney TF, Sindelar WF, Tochner Z, Smith PD, Friauf WS, Thomas GF, Dachowski LJ, Cole JW, Steinberg SM, Glatstein E. Phase I study of debulking surgery and photodynamic therapy for disseminated intraperitoneal tumors. Int J Radiat Oncol Biol Phys 1993;25:445–457.
2. Sindelar WF, DeLaney TF, Tochner Z, Thomas GF, Dachowski LJ, Smith PD, Friauf WS, Cole JW, Glatstein E. Technique of photodynamic therapy for disseminated intraperitoneal malignant neoplasms. Phase I study. Arch Surg 1991;126:318–324.
3. Lilge L, Molpus K, Hasan T, Wilson BC. Light dosimetry for intraperitoneal photodynamic therapy in a murine xenograft of human epithelial ovarian carcinoma. Photochem Photobiol 1998;68:281–288.
4. Veenhuizen RB, Ruevekamp MC, Oppelaar H, Ransdorp B, van de Vijver M, Helmerhorst TJ, Kenemans P, Stewart FA. Intraperitoneal photodynamic therapy: comparison of red and green light distribution and toxicity. Photochem Photobiol 1997;66:389–398.
5. Wilson BC, Patterson MS, Lilge L. Implicit and explicit dosimetry in photodynamic therapy: a new paradigm. Lasers Med Sci 1997;12:182–199.
6. Georgakoudi I, Nichols MG, Foster TH. The mechanism of Photofrin photobleaching and its consequences for photodynamic dosimetry. Photochem Photobiol 1997;65:135–144.
7. Wilson BC, Patterson MS. The physics of photodynamic therapy. Phys Med Biol 1986;31:327–360.
8. Cheong WF, Prahl SA, Welch AJ. A review of the optical properties of biological tissues. IEEE J Quant Elect 1990; 26:2166–2185.
9. Van Staveren HJ, Marijnissen JPA, Aalders MCG, Star WM. Construction, quality assurance and calibration of spherical isotropic fibre optic light diffusers. Lasers Med Sci 1995;10:137–147.
10. Marijnissen JPA, Star WM. Calibration of isotropic light dosimetry probes based on scattering bulbs in clear media. Phys Med Biol 1996;41:1191–1208.
11. Baas P, Murrer LHP, Zoetmulder FAN, Stewart FA, Ris HB, van Zandwijk N, Rutgers EM. Photodynamic therapy as adjunctive in surgically treated pleural malignancies. Br J Cancer 1997;76:819–826.
12. Star WM. Light dosimetry in vivo. Phys Med Biol 1997; 42:763–787.
13. Friauf WS, Smith PE, Russo A, DeLaney TF, Pass HI, Cole JW, Gibson CC, Sindelar WF, Thomas G. Light monitoring in photodynamic therapy. In: Nagle HR, Tomkins WJ, editors. IEEE case studies in medical instrument design. New York; 1992. p 127–138.
14. Martelli F, Sassaroli A, Zaccanti G, Yamada Y. Properties of the light emerging from a diffusive medium: angular dependence and flux at the external boundary. Phys Med Biol 1999;44:1257–1275.
15. Farrell J, Patterson MS, Wilson B. A diffusion theory model of spatially resolved, steady-state diffuse reflectance for the noninvasive determination of tissue optical properties in vivo. Med Phys 1992;19:879–883.
16. Mendenhall W. Introduction to probability and statistics. Boston: PWS Publishers; 1983.
17. Yodh A, Chance B. Spectroscopy and imaging with diffusing light. Physics Today 1995;48:34–40.